The EMBO Journal Vol.18 No.11 pp.2923–2929, 1999

The crystal structure of the *Physarum polycephalum* actin–fragmin kinase: an atypical protein kinase with a specialized substrate-binding domain

Stefan Steinbacher[1], Peter Hof, Ludwig Eichinger[2], Michael Schleicher[2], Jan Gettemans[3], Joël Vandekerckhove[3], Robert Huber and Jörg Benz[4]

Abteilung Strukturforschung, Max-Planck-Institut für Biochemie, 82152 Martinsried, [2]A.-Butenandt-Institut/Zellbiologie, Ludwig-Maximilians-Universität, 80336 München, Germany and [3]Flanders Interuniversity Institute of Biotechnology, University of Gent, 9000 Gent, Belgium

[4]Present address: Department für Chemie und Biochemie, Universität Bern, 3012 Bern, Switzerland

[1]Corresponding author
e-mail: steinbac@biochem.mpg.de

Coordinated temporal and spatial regulation of the actin cytoskeleton is essential for diverse cellular processes such as cell division, cell motility and the formation and maintenance of specialized structures in differentiated cells. In plasmodia of *Physarum polycephalum*, the F-actin capping activity of the actin–fragmin complex is regulated by the phosphorylation of actin. This is mediated by a novel type of protein kinase with no sequence homology to eukaryotic-type protein kinases. Here we present the crystal structure of the catalytic domain of the first cloned actin kinase in complex with AMP at 2.9 Å resolution. The three-dimensional fold reveals a catalytic module of ~160 residues, in common with the eukaryotic protein kinase superfamily, which harbours the nucleotide binding site and the catalytic apparatus in an inter-lobe cleft. Several kinases that share this catalytic module differ in the overall architecture of their substrate recognition domain. The actin–fragmin kinase has acquired a unique flat substrate recognition domain which is supposed to confer stringent substrate specificity.

Keywords: actin phosphorylation/crystal structure/cytoskeleton reorganization/fragmin/protein kinase

Introduction

Protein phosphorylation plays a key role in regulating the dynamic rearrangements of the cytoskeleton starting with upstream signalling cascades (Eby *et al*., 1998) resulting in phosphorylation of downstream effectors which directly interact with actin or tubulin. For example, the signalling pathway of Rac-mediated stimulus-induced actin reorganization results in phosphorylation of cofilin by LIM-kinase (Arber *et al*., 1998) which abolishes cofilin's actin binding and depolymerization activities (Arber *et al*., 1998; Yang *et al*., 1998). Phosphorylation of actin itself has been observed repeatedly. Treatment of mammalian cells with epidermal growth factor induces rapid phosphorylation of actin in the cortical skeleton (van Delft *et al*., 1995). Stage-dependent phosphorylation of actin at Tyr53 in *Dictyostelium discoideum* (Howard *et al*., 1993; Jungbluth *et al*., 1995) is associated with morphological alterations and reorganization of the actin cytoskeleton.

Plasmodial fragmin from the slime mould *Physarum polycephalum* is a member of the gelsolin family which has been implicated in cellular processes that require rapid actin cytoskeleton reorganization, and interferes with the growth of F-actin by severing actin filaments and capping their barbed ends. The EGTA-resistant 1:1 complex between actin and fragmin has been identified as the sole *in vivo* target for a specific protein kinase (actin–fragmin kinase, AFK) that phosphorylates actin mainly at Thr203 and to a minor extent at Thr202 in the actin–fragmin complex but not in G-actin (Gettemans *et al*., 1992; De Corte *et al*., 1996). The phosphorylation sites are located at the minor contact site for DNase I (Kabsch *et al*., 1990) and at one of the proposed actin–actin contact sites along the long-pitch helix of F-actin (Holmes *et al*., 1990). The F-actin nucleating activity of actin–fragmin is abolished upon phosphorylation *in vitro* and its capping activity becomes Ca^{2+}-dependent. The latter observation was corroborated by microinjection of the (un)phosphorylated actin–fragmin complex in mammalian cells (Constantin *et al*., 1998). These data indicate that actin polymerization in *Physarum* can be controlled by actin phosphorylation in a Ca^{2+}-dependent manner.

Biochemical studies and cloning of the AFK resulted in the identification of an 80 kDa protein representing a novel type of protein kinase (Eichinger *et al*., 1996). Two domains of ~35 kDa are linked by a sequence stretch of 50 amino acids rich in proline and serine residues. Whereas the C-terminal part harbours six so-called 'kelch'-repeats, indicating a six-bladed propeller structure (Bork and Doolittle, 1994), the N-terminal part consists of a catalytically active protein kinase domain (cAFK) which, most notably, does not show any sequence similarities to eukaryotic protein kinases and lacks all signature motifs that characterize this super-family (Hanks and Hunter, 1995; Eichinger *et al*., 1996). Here we report on the crystal structure of cAFK that was solved to gain insight into the structural basis of phosphoryl transfer and potential structural relationships to typical protein kinases.

Results and discussion

Overall structure

Recombinant cAFK was crystallized from high salt conditions in the presence of AMP. Other nucleotides or nucleotide analogues did not give crystals suitable for structure determination. The structure was solved by single isomorphous replacement and two-fold non-crystallographic symmetry averaging. The structure has been refined to a crystallographic *R*-factor of 19.9% and R_{free}

Table I. Data collection, phasing and refinement statistics

Data collection and phasing	Limiting resolution (Å)	Unique reflections	Mean redundancy	Completeness (%)	R_{sym} (%)	R_{iso} (%)	Phasing power	R_C
NATI	2.9	23 306	2.7	94.9 (77.4)	8.0 (41.9)	–	–	–
PCMB	3.3	16 028	2.3	97.7 (38.5)	16.2 (83.4)	21.4	1.93	0.63

Refinement statistics	Non-hydrogen atoms	Reflections used	R_{work} (%)	R_{free} (%)	r.m.s. bond length (Å)	r.m.s. bond angle (°)	r.m.s. bonded B (Å^2)	r.m.s. ncs atoms (Å)
NATI	5148	22 289	19.8	27.2	0.011	1.82	3.43	0.31

NATI: 15.0–2.9 Å (3.06–2.90 Å); PCMB 15.0–3.3 Å (anomalous completeness). PCMB: 4 mM *p*-chloromercuribenzoic acid, 18 h.
$R_{sym} = \Sigma|I-<I>|/\Sigma I$, where I = observed intensity, $<I>$ = average intensity from multiple observation. $R_{iso} = \Sigma||F_{PH}|-|F_P||/\Sigma|F_P|$, where $|F_P|$ = protein structure factor amplitude, $|F_{PH}|$ = heavy-atom derivative structure factor amplitude. Phasing power = r.m.s. ($|F_H|/E$), where F_H = heavy-atom structure factor amplitude and E = residual lack of closure.
$R_C = \Sigma|F_{PH} \pm F_P - F_{Hcalc}|/\Sigma|F_{PH} \pm F_P|$ (centric reflections).

of 27.2% using data in the resolution shell from 8.0 to 2.9 Å (see Materials and methods; Table I). The model incorporates residues 2–343 and one AMP molecule; residues 33–47 are not defined by electron density. cAFK has overall dimensions of ~30×50×60 Å and is comprised of eight β-strands (S1–S8) and 11 α-helices (H1–H11), organized in two lobes (Figure 1). The 165-residue N-terminal lobe consists of four α-helices (H1–H4) and a five-stranded, anti-parallel β-sheet (S1–S5) of topology 1-2-3-5-4. Helices H3 and H4 are inserted between β-strands S4 and S5, and helix H2 is between S3 and S4. The β-strand S1 is preceded by 72 residues that wrap around the back side of the N-lobe with a loop structure that is located at the side entrance of the nucleotide-binding cleft and connects the N- and C-lobe, including 14 disordered residues. Helices H3 and H4 pack against the β-sheets of the N-lobe. The N-terminal helix H1 packs against H2 of the N-lobe and H10 of the C-lobe. A hinge region at the bottom of the nucleotide binding-cleft is located between β-strands S5 and S6 and connects the N- and C-lobe. The 178-residue C-terminal lobe consists of the remaining seven α-helices (H5–H11) and a three-stranded, anti-parallel β-sheet (S6–S8) of topology 6-7-8. Helices H5 and H6 are inserted between β-strands S6 and S7. β-strand S8 is followed by helices H7–H11 which contact helices H1, H2, H5 and H6, completing an arch of nine α-helices that surrounds one side of the nucleotide-binding cleft and packs against the β-sheet of the C-lobe.

Conserved catalytic core

Comparison of cAFK to the catalytic subunit of cAMP-dependent protein kinase (cAPK) (Knighton *et al*., 1991; Bossemeyer *et al*., 1993) as a prototype of eukaryotic protein kinases reveals a topologically equivalent region which is common to both kinases (Figures 1 and 2). This region spans residues 73–232 in cAFK and includes the secondary structure elements from S1 to S8. Helices H2 and H6 correspond to helices C and E in cAPK. This corresponds to subdomains 1–7 in eukaryotic protein kinases and comprises a minimal kinase module that contains all elements necessary for phosphoryl transfer. The cAFK and cAPK structures diverge C-terminal to Asp232, which corresponds to Asp184 of the DFG motif. A structure-based sequence comparison results in a sequence identity as low as 14% using 76 topologically equivalent residues out of 159 residues of the subdomains in common. The highest local similarity is observed for the hinge region between N- and C-lobe (cAFK: MELVRG; cAPK: MEYVPG) although this region does not represent a signature sequence in typical protein kinases. In particular, the signature sequences (Hanks and Hunter, 1995) H/Y-R-D-L/I-K-P-X-N for Ser/Thr kinases, H-R-D-L-R/A-A-A/R-N for tyrosine kinases of the catalytic loop, G-X-G-X-X-G of the glycine rich loop or the well known DFG motif preceding the activation segment are not observed in cAFK. These regions deviate structurally from all other known protein kinases. The glycine rich loop connecting β-strands S1 and S2 is shorter by one residue in cAFK. The catalytic loop in cAFK that ranges from Asp204 to Asn218 (corresponding to Asp166 and Asn171) bears an insertion of nine residues providing contacts with helices H8 and H9, and is therefore of structural importance, but it also protrudes from the otherwise flat surface.

Weak autophoshorylation has been observed for recombinant AFK (Eichinger *et al*., 1996), but it is unknown whether the region corresponding topologically to the activation loop has an analogous function. There are two serine residues, Ser233 and Ser241, in the coil region connecting β-strand S8 and helix H7 that could be potential candidates for autophosphorylation. The distance of nine residues between the beginning of the activation segment and Ser241 would correspond to that observed in other kinases (Hanks and Hunter, 1995). High temperature factors are observed for the residue range from Ile236 to Arg249, which involves the activation segment and the N-terminal half of helix H7 with the highest temperature factors being found in both asymmetric monomers around Ser241. This indicates potential flexibility compatible with regulatory functions for this region.

Phosphoryl transfer

Superimposing the adenine moiety in cAFK and cAPK reveals an analogous mode of nucleotide binding. The adenine is located between Ile96 from β-sheet S3 and Met220 from S7, and occupies a mostly hydrophobic pocket between both lobes. Other residues include Leu85, Phe87, Pro121, Met162 and Ile231 with the connecting hinge region at the base of the cleft. Polar van der Waals contacts are made with the backbone in the hinge region with a hydrogen bond of the N6 amino group to the carbonyl group of Glu163. The ribose forms only van der Waals contacts to O_γ of Ser78 of the N-lobe, and to the

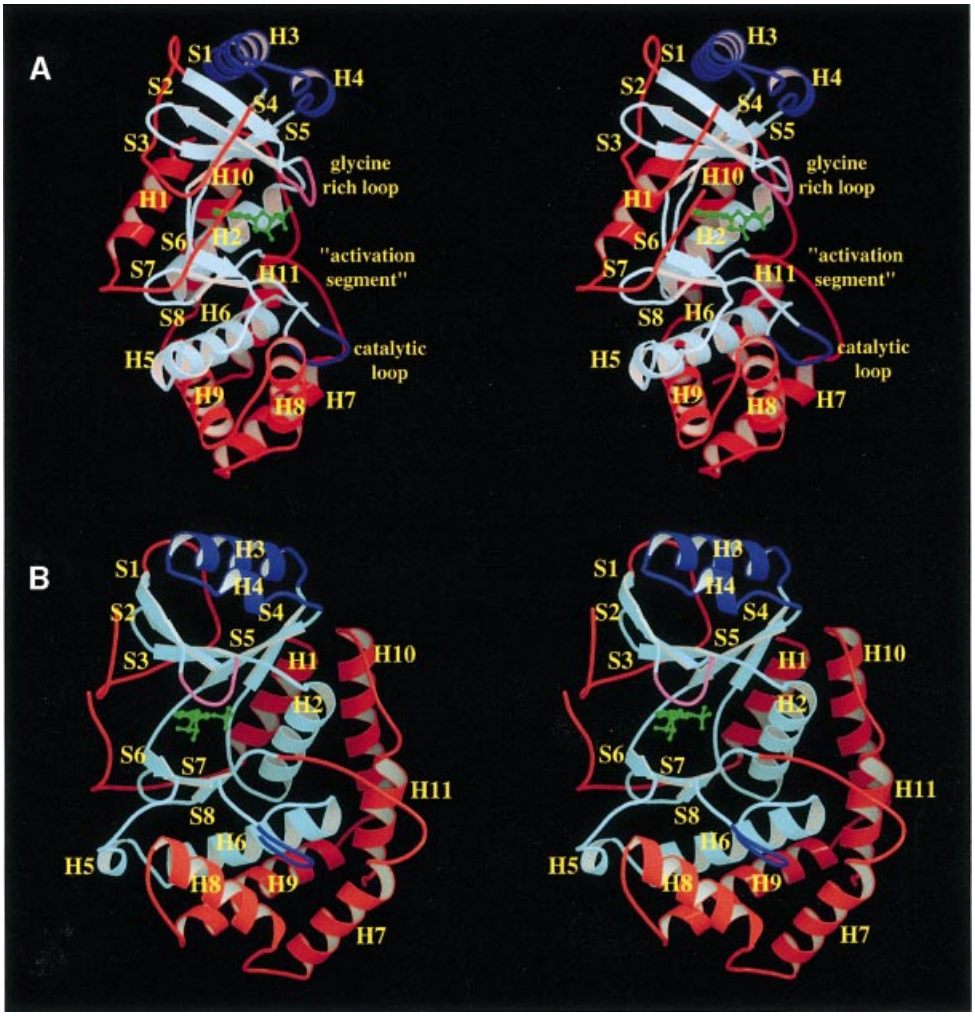

C

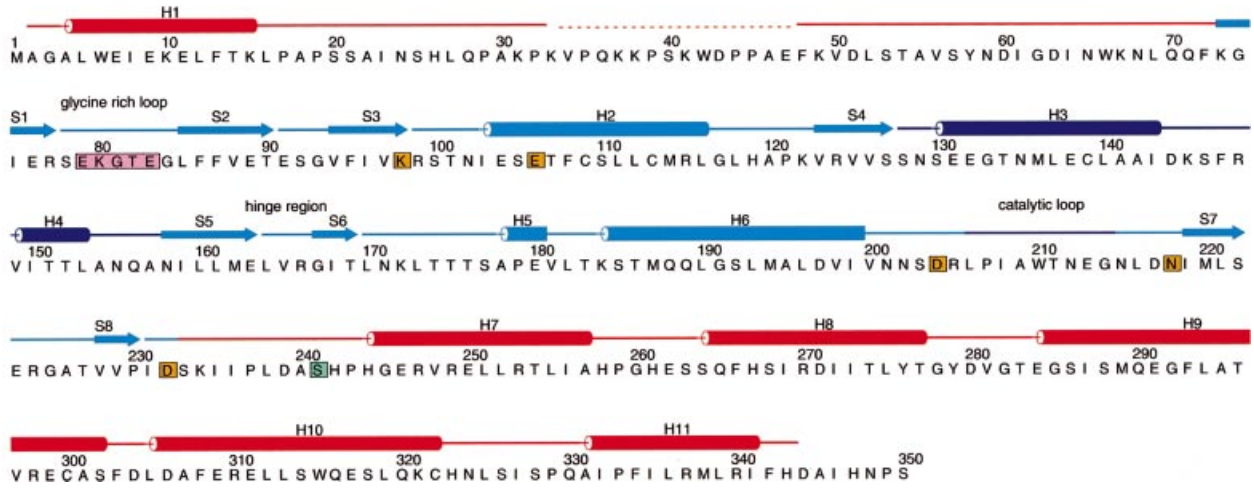

Fig. 1. (**A**) Ribbon diagram of the catalytic domain of actin–fragmin kinase (cAFK). View into the nucleotide-binding cleft with bound AMP depicted in green. The N-lobe is located above, the C-lobe below this cleft. Helices are labelled H1–H11, β-strands S1–S8. The catalytic kinase module, in common with eukaryotic-type protein kinases (ePKs), is coloured in light blue. Parts of the kinase module that differ from ePKs are shown in dark blue, including helices H3 and H4 and the insertion into the catalytic loop. Parts that topologically differ from ePKs are shown in red. (**B**) Perpendicular view to (A) as seen from the right side. (**C**) Sequence and secondary structure of cAFK. Conserved catalytic residues are shaded in yellow, the glycine rich loop in magenta, a potential site of autophosphorylation in green. Colour coding of secondary structural elements as in (A).

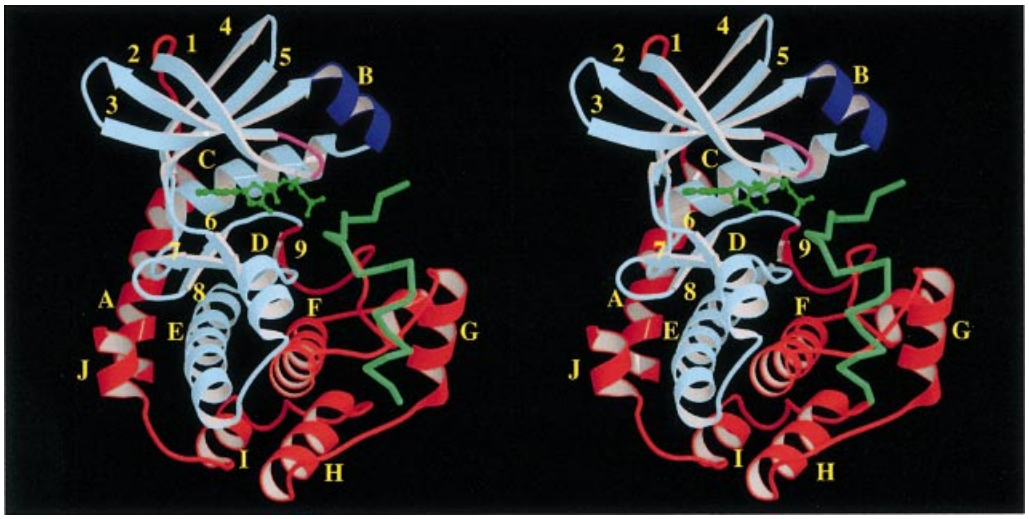

Fig. 2. Crystal structure of cAPK with bound ATP (green) and PKI-inhibitor fragment (light green) for comparison. Orientation is with aligned nucleotides in the kinase modules as in Figure 1A. Colour coding as in Figure 1. Helices are labelled A–J, β-sheets 1–9. The peptide inhibitor is bound to a richly structured cleft with its N-terminal part. The main contacts involve helices D, F, G and H. These parts are absent in cAFK that has a flat substrate recognition surface (compare with Figure 1).

side chain of Thr169 and the carbonyl group of Asp217 from the C-lobe. The glycine rich loop helps to position the phosphate by formation of a hydrogen bond to the backbone amide of Thr82, although it probably adopts an arbitrary conformation in the presence of AMP, resulting in high temperature factors and a less well-defined electron density. This loop has been reported to be a relatively flexible element in other kinases as well (Cox *et al*., 1994) and its stability highly depends on bound ligands. The same is true for the inter-lobe angle which indicates either an open (inactive) or closed (active) state.

Five strictly conserved residues are found in the active site of cAFK compared with the protein kinase superfamily, and these have been identified as being essential for catalysis (Figure 3) (residue numbers for cAPK in parentheses): Lys98 (72), Glu106 (91), Asp204 (166), Asn218 (171) and Asp232 (184). Lys98 contacts the α-phosphate of AMP, the corresponding residue in cAPK additionally contacts the β-phosphate of the bound nucleotide. Lys98 forms a conserved salt bridge with Glu106. The catalytic loop harbours Asp204 and Asn218. Asp166 in cAPK interacts with the incoming substrate and is thought to act as a base required for deprotonation of the substrate hydroxyl group enabling efficient hydrolytic attack at the γ-phosphate. Asn171 binds to a second divalent metal ion. The α-phosphate of AMP makes contacts to Asp232. The role of the analogous Asp184 of the DFG motif in cAPK involves binding of the Mg^{2+} ion that bridges the β- and γ-phosphate.

Specialized substrate-binding domain

The substrate-binding regions of typical protein kinases are well established (Johnson *et al*., 1998), by inhibitor binding in cAPK (Knighton *et al*., 1991; Bossemeyer *et al*., 1993), and by pseudosubstrate-like binding in twitchin kinase (Hu *et al*., 1994) or calcium/calmodulin-dependent protein kinase I (Goldberg *et al*., 1996). The N-terminal part of the substrate analogue is bound to a channel on the surface of the protein that is created by the edge of helix D along with an extensive region stretching from the end of helix F through helices G and H (Figure 2). The precise orientation of the substrate analogue varies as it is observed for the orientation of helix D. These structural elements belong to subdomains 5, 9 and 10 in the primary structure of typical protein kinases. The region following the DFG motif, subdomain 8, comprising the activation segment, appears to play a major role in recognition of peptide substrates in cAPK. These structural elements are absent in cAFK including helix D that topologically belongs to the kinase module. Based on the binding mode of the PKI fragment in the active site cleft of the catalytic module of cAPK, the phosphorylated loop around Thr203 in subdomain 4 of actin can be docked into the active site cleft of cAFK and allows the prediction of regions potentially important for substrate interaction. A remarkable complementarity in shape thus emerges, that allows docking of actin into the catalytic loop through the cleft between subdomains 2 and 4 of actin, exposing Thr211 and Glu213 of cAFK. The 'activation segment', the C-terminus of helix H6 and the N-terminal half of helix H7 of cAFK would contact the third β-strand (from Leu65 to Lys68) at the edge of a β-pleated sheet of actin subdomain 2 (Kabsch *et al*., 1990). Helix H8 of cAFK would face the first helix (from Gly182 to Thr194) in subdomain 4 of actin (Figure 4). The catalytic loop insertion and the surrounding helices H6, H7 and H8 therefore probably form a relatively flat substrate recognition domain that diverges significantly from the elaborately structured substrate recognition domain in eukaryotic protein kinases (Figures 1 and 2). Since only the structure of gelsolin segment-1 in complex with actin is known (McLaughlin *et al*., 1993), where segment-1 binds to a cleft between subdomains 1 and 3, the role of fragmin, fragmin60 (Furuhashi *et al*., 1989, 1992) or *Dictyostelium* severin in substrate recognition by cAFK remains unclear. However, this structure shows that the phosphorylated loop around Thr203 is considerably flexible in comparison to the actin–DNase I complex, and this may explain why neighbouring threonine residues in actin can also be

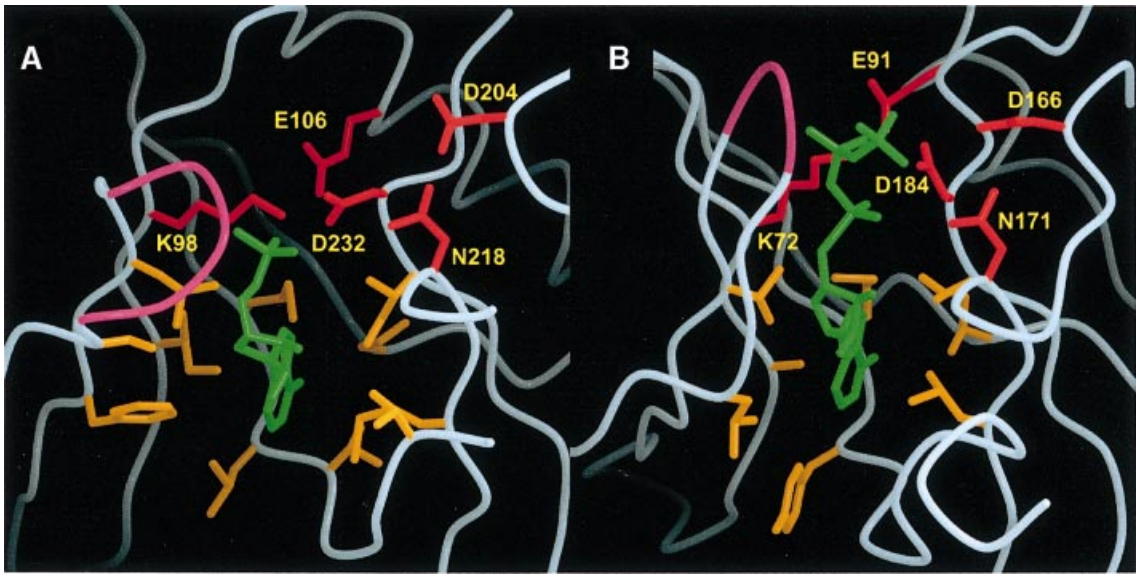

Fig. 3. Comparison of the actives site of cAFK (**A**) and cAPK (**B**). The orientation corresponds approximately to a 90° counterclockwise rotation compared with Figure 1A. (A) The N-lobe is located on the left side, the C-lobe on the right side. Hydrophobic residues that form the adenine binding pocket are in orange, bound AMP in green and strictly conserved catalytic residues compared with typical eukaryotic protein kinases in red. The glycine rich loop contacting the α-phosphate is shown in magenta, (B) cAPK colour coding as in (A). The catalytic mechanism of phosphoryl transfer by the kinase module appears to be strictly preserved throughout evolution, even in very distant relatives that have acquired completely different substrate-binding modes.

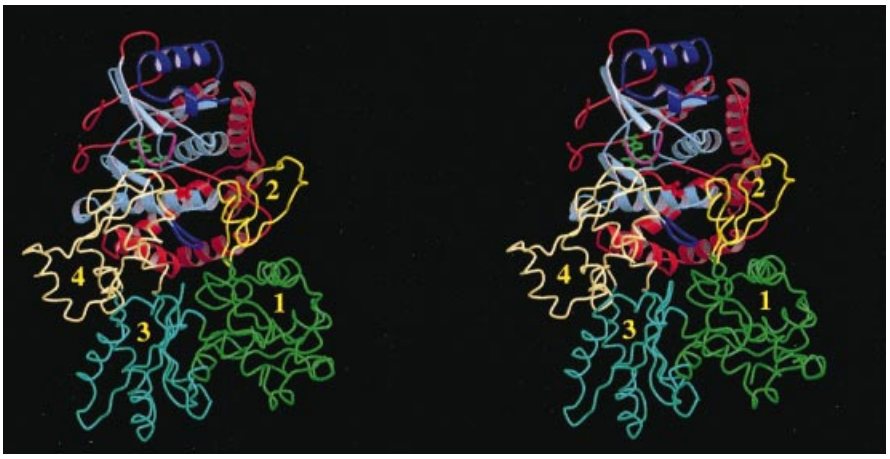

Fig. 4. Proposed interaction of cAFK and actin. Actin coordinates were taken from the actin–DNase I complex (Kabsch *et al*., 1990). Subdomains 1–4 of actin are shown as wire, the orientation of cAFK is similar to Figure 1B. The phosphorylated loop of actin in subdomain 4 (coloured in red) was docked into the active site, the phosphorylated residue Thr203 is shown as ball-and-stick model. Subdomain 2 of actin is predicted to interact with helices H7 and H11 and the 'activation segment', subdomain 4 mainly with helices H6 and H8. The insertion into the catalytic loop of cAFK (dark blue) is complementary to the cleft between subdomains 2 and 4 of actin and therefore probably essential for specific recognition of actin. As gelsolin segment-1 binds to the cleft between subdomain 1 and 3 of actin, complete fragmin is expected to provide additional contacts between the substrate complex (actin–fragmin) and AFK.

phosphorylated (Furuhashi *et al*., 1992; Gettemans *et al*., 1992).

Conclusion

This analysis shows that the atypical actin–fragmin kinase from *P.polycephalum*, which phosphorylates actin only when actin is complexed with plasmodial fragmin, bears a structural relationship to the eukaryotic-type protein kinase family with respect to the kinase module. A clue to the observed specificity can be deduced from the unique substrate binding domain that appears to be complementary to the inter-lobe cleft of actin. This substrate binding domain discriminates AFK from the eukaryotic-type kinase superfamily.

Other divergent representatives of the protein kinase superfamily have recently been observed in small molecule kinases. The microbial aminoglycoside kinase APH(3′)-IIIa catalyses the phosphorylation of a broad spectrum of aminoglycoside antibiotics (Hon *et al*., 1997). Its structure can roughly be superimposed in parts of the secondary structure elements on subdomains 1–9, ranging from β-sheet 1 to helix F in cAPK. Approximately the same region is encountered in the type IIβ phosphatidylinositol phosphate kinase (Rao *et al*., 1998), a lipid kinase with a

critical role in eukaryotic signal transduction pathways. These structures demonstrate that a considerably smaller part, the kinase module, is sufficient for binding ATP and phosphorylating the substrate.

The structurally conserved character of features that are essential for phosphoryl transfer, identified in a number of protein kinases, suggests a stringently conserved mechanism of phosphoryl transfer associated with the ubiquitous kinase module. The conserved topology of the catalytic core and the variability in substrate recognition observed in cAFK, eukaryotic-type protein kinases, APH(3′)-IIIa, and IIβ phosphatidylinositol phosphate kinase, suggest divergent evolution from an ancestral kinase. Specific requirements for substrate recognition as in AFK, or a flat interface for membrane interaction as in phosphatidylinositol phosphate kinase (Rao *et al*., 1998), have resulted in specialized substrate-binding domains.

The pronounced role of eukaryotic-type protein kinases in signal tranduction in highly specialized and differentiated cells of multicellular organisms can be seen as the major driving force underlying their enormous diversity. As a result, they have evolved into one of the largest protein families, comprising ~1% of the human genome (Hanks and Hunter, 1995), but have retained most features of substrate recognition surprisingly well. However, as illustrated by the actin–fragmin kinase, substrate recognition can be much more diverse in true protein kinases than previously observed. Based on these structural findings one may predict that other unusual protein kinases (Hanks and Hunter, 1995) are also structurally related to the eukaryotic protein kinase superfamily.

Materials and methods

Recombinant cAFK was expressed in *Escherichia coli* and purified as described previously (Eichinger *et al*., 1996). The protein was dialysed against 10 mM MES/NaOH pH 7.5, and concentrated to 10 mg/ml. For crystallization 5 µl of the protein solution were mixed with 2 µl of a 10 mM stock solution AMP and 5 µl of 2.0 M Li_2SO_4 in 100 mM MES/NaOH pH 6.0, and equilibrated over 2.0 M Li_2SO_4. Trigonal crystals of space group P3(2)21 with $a = b = 178.9$ Å, $c = 59.3$ Å, $\alpha = \beta = 90°$ and $\gamma = 120°$ grew within 1 week to a maximum final size of 0.4 mm.

X-ray diffraction data were collected on a Mar research imaging plate detector mounted on a Rigaku rotating anode X-ray generator, operating at 50 kV and 100 mA. Measured intensities were integrated with MOSFLM (Leslie, 1991) and scaled and merged using the CCP4 program suite (Collaborative Computational Project, 1994). A heavy atom derivative was prepared by soaking a crystal in 4 mM of *p*-chloromercuribenzoic acid for 18 h. Seven heavy atom sites were identified with SHELXS (Sheldrick *et al*., 1993). Heavy atom parameters were refined with MLPHARE (Collaborative Computational Project, 1994). The mean figure of merit was 0.34.

The 3.3 Å electron density was improved by solvent flattening (68% solvent content) with DM (Collaborative Computational Project, 1994). The NCS operators for two-fold non-crystallographic averaging were derived from a partial model and improved with the programme IMPROVE (Kleywegt and Jones, 1993). Cyclic averaging with RAVE (Kleywegt and Jones, 1993) resulted in a back-transformation *R*-factor $R_{back} = 17.1\%$. The resulting electron density was of superb quality. The complete model for one monomer and the AMP molecule could be traced in the first round of model building with the programme FRODO (Jones, 1978). The structure was refined with X-PLOR (Brünger, 1992). A test set of 5% of the reflections was used for cross-validation. NCS constraints were applied to the atomic positions (r.m.s.d. of 0.31 Å for all atoms) but not to temperature factors as protomer A had a significantly lower average *B*-factor (44.0 $Å^2$) than protomer B (66.1 $Å^2$). A bulk solvent correction was applied in the final stages as implemented in X-PLOR with $|F| > 2\sigma|F|$ in the resolution range 15.0–2.9 Å. The structure displays good stereochemical parameters as estimated by the programme PROCHECK (Laskowski *et al*., 1993) with 86.7% in the most favoured region and 11.6 in additionally allowed regions in a Ramachandran plot (Ramachandran and Sasisekharan, 1968).

Accession code

The coordinates have been deposited with the Protein Data Bank with the accession code 1cjg.

Acknowledgements

This work was supported by the Deutsche Forschungsgemeinschaft, Sonderforschungsbereich 413 and the Fonds der Chemischen Industrie. J.G. is a Postdoctoral Fellow of the Fund for Scientific Research-Flanders (Belgium) (F.W.O.).

References

Arber,S., Barbayannis,F.A., Hanser,H., Schneider,C., Stanyon,C.A., Bernard,O. and Caroni,P. (1998) Regulation of actin dynamics through phosphorylation of cofilin by LIM-kinase. *Nature*, **393**, 805–809.

Bork,P. and Doolittle,R.F. (1994) *Drosophila* kelch motif is derived from a common enzyme fold. *J. Mol. Biol.*, **236**, 1277–1282.

Bossemeyer,D., Engh,R.A., Kinzel,V., Ponstingl,H. and Huber,R. (1993) Phosphotransferase and substrate binding mechanism of the cAMP-dependent protein kinase catalytic subunit from porcine heart as deduced from the 2.0 Å structure of the complex with Mn^{2+} adenylyl imidodiphosphate and inhibitor peptide PKI(5–24). *EMBO J.*, **12**, 849–859.

Brünger,A. (1992) *X-PLOR version 3.1. A System for Crystallography and NMR*. Yale University Press, New Haven, CT.

Collaborative Computational Project, 4 (1994) The CCP4 suites: programs for protein crystallography. *Acta Crystallogr.*, **D50**, 760–763.

Constantin,B., Meerschaert,K., Vandekerckhove,J. and Gettmans,J. (1998) Disruption of the actin cytoskeleton of mammalian cells by the capping complex actin–fragmin is inhibited by actin phosphorylation and regulated by Ca^{2+} ions. *J. Cell Sci.*, **111**, 1695–1706.

Cox,S., Radzio-Andzelm,E. and Taylor,S.S. (1994) Domain movements in protein kinases. *Curr. Opin. Struct. Biol.*, **4**, 893–901.

De Corte,V., Gettemans,J., Waelkens,E. and Vandekerckhove,J. (1996) *In vivo* phosphorylation of actin in Physarum polycephalum. Study of the substrate specificity of the actin–fragmin kinase. *Eur. J. Biochem.*, **241**, 901–908.

Eby,J.J., Holly,S.P., van Drogen,F., Grishin,A.V., Peter,M., Drubin,D.G. and Blumer,K.J. (1998) Actin cytoskeleton organization regulated by the PAK family of protein kinases. *Curr. Biol.*, **8**, 967–970.

Eichinger,L., Bomblies,L., Vandekerckhove,J., Schleicher,M. and Gettemans,J. (1996) A novel type of protein kinase phosphorylates actin in the actin–fragmin complex. *EMBO J.*, **15**, 5547–5556.

Furuhashi,K., Hatano,S., Ando,S., Nishizawa,K. and Inagaki,M. (1992) Phosphorylation by actin kinase of the pointed end domain on the actin molecule. *J. Biol. Chem.*, **267**, 9326–9330.

Furuhashi,K. and Hatano,S. (1989) A fragmin-like protein from plasmodium of *Physarum polycephalum* that severs F-actin and caps the barbed end of F-actin in a Ca^{2+}-sensitive way. *J. Biochem. (Tokyo)*, **106**, 311–318.

Gettemans,J., De Ville,Y., Vandekerckhove,J. and Waelkens,E. (1992) *Physarum* actin is phosphorylated as the actin–fragmin complex at residues Thr203 and Thr202 by a specific 80 kDa kinase. *EMBO J.*, **11**, 3185–3191.

Goldberg,J., Nairn,A.C. and Kuriyna,J. (1996) Structural basis for the autoinhibition of calcium/calmodulin-dependent protein kinase I. *Cell*, **84**, 875–887.

Hanks,S.K. and Hunter,T. (1995) The eukaryotic protein kinase superfamily: kinase (catalytic) domain structure and classification. *FASEB J.*, **9**, 576–596.

Holmes,K.C., Popp,D., Gebhard,W. and Kabsch,W. (1990) Atomic model of the actin filament. *Nature*, **347**, 44–49.

Hon,W.-C., McKay,G.A., Thompson,P.R., Sweet,R.M., Yang,D.S.C., Wright,G.D. and Berghuis,A.M. (1997) Structure of an enzyme required for aminoglycoside antibiotic resistance reveals homology to eukaryotic protein kinases. *Cell*, **89**, 887–895.

Howard,P.K., Sefton,B.M. and Firtel,R.A. (1993) Tyrosine phosphorylation of actin in *Dictyostelium* associated with cell-shape changes. *Science*, **259**, 241–244.

Hu,S.-H., Parker,M.W., Lei,J.Y., Wilice,M.C.J., Benian,G.M. and Kemp,B.E. (1994) Insight into autoregulation from the crystal structure of twitchin kinase. *Nature*, **369**, 581–584.

Johnson,L.N., Lowe,E.D., Noble,M.E.M. and Owen,D.J. (1998) The structural basis for substrate recognition and control by protein kinases. *FEBS Lett.*, **430**, 1–11.

Jones,T.A. (1978) A graphics model building and refinement system for macromolecules. *J. Appl. Crystallogr.*, **11**, 268–272.

Jungbluth,A., Eckerskorn,C., Gerisch,G., Lottspeich,F., Stocker,S. and Schweiger,A. (1995) Stress-induced tyrosine phosphorylation of actin in *Dictyostelium* cells and localization of the phosphorylation site to tyrosine-53 adjacent to the DNase I binding loop. *FEBS Lett.*, **375**, 87–90.

Kabsch,W., Mannherz,H.G., Suck,D., Pai,E.F. and Holmes,K.C. (1990) Atomic structure of the actin DNase I complex. *Nature*, **347**, 37–44.

Kleywegt,G.J. and Jones,T.A. (1993) Mask made easy. *ESF/CCP4 Newsletter*, **28**, 56–59.

Knighton,D.R., Zheng,J.H., Ten Eyck,L.F., Ashford,V.A., Xuong,N.H., Taylor,S.S. and Sowadski,J.M. (1991) Crystal structure of the catalytic subunit of cyclic adenosine monophosphate-dependent protein kinase. *Science*, **253**, 407–414.

Laskowski,R.A., MacArthur,M.W., Moss,D.S. and Thornton,J.M. (1993) PROCHECK: a program to check the stereochemical quality of protein structures. *J. Appl. Crystallogr.*, **26**, 283–291.

Leslie,A.G.W. (1991) *Recent Changes to the MOSFLM Package for Processing Film and Image Plate Data*. SERC Laboratory, Daresbury, Warrington WA44AD, UK.

McLaughlin,P.J., Gooch,J.T., Mannherz,H.-G. and Weeds,A.G. (1993) Structure of gelsolin segment 1–actin complex and the mechanism of filament severing. *Nature*, **364**, 685–692.

Ramachandran,G.N. and Sasisekharan,V. (1968) Conformation of polypeptides and proteins. *Adv. Protein Chem.*, **23**, 283–438.

Rao,V.D., Misra,S., Boronenkov,I.V., Anderson,R.A. and Hurley,J.H. (1998) Structure of type IIb phosphatidylinositol phosphate kinase: a protein kinase fold flattened for interfacial phosphorylation. *Cell*, **94**, 829–839.

Sheldrick,G.M., Dauter,Z., Wilson,K.S., Hope,H. and Sieker,L.C. (1993) The application of direct methods of patterson interpretation to high-resolution native protein data. *Acta Crystallogr.*, **D49**, 18–23.

van Delft,S., Verkleij,A.J., Boonstra,J. and van Bergen en Henegouwen, P.M.P. (1995) Epidermal growth factor induces serine phosphorylation of actin. *FEBS Lett.*, **357**, 251–254.

Yang,N., Higuchi,O., Ohashi,K., Nagata,K., Wada,A., Kangawa,K., Nishida,E. and Mizuno,K. (1998) Cofilin phosphorylation by LIM-kinase 1 and its role in Rac-mediated actin reorganization. *Nature*, **393**, 809–812.

Received March 9, 1999; revised and accepted April 7, 1999